International Journal of Innovative Computing, Information and Control
Volume **19**, Number **1**, February **2023**

ICIC International ©2023 ISSN 1349-4198
pp. **101–121**

SECURING A SYNCHRONIZATION ZONE TO REALIZE A HIGH EFFICIENCY PRODUCTION BASED ON THE GENERALIZED THEORY OF RELATIVITY

Kenji Shirai[1], Yoshinori Amano[2], Atsuya Ando[1] and Takayuki Uda[1]

[1]Faculty of Business and Informatics
Niigata University of International and Information Studies
3-1-1, Mizukino, Nishi-ku, Niigata 950-2292, Japan
dr.kenji5761@gmail.com; { atsuya; uda }@nuis.ac.jp

[2]Kyohnan Elecs Co., LTD.
8-48-2, Fukakusanishiura-cho, Fushimi-ku, Kyoto 612-0029, Japan
y_amano@kyohnan-elecs.co.jp

Received June 2022; revised September 2022

Abstract. *We have pointed out that process synchronization is essential to the production processes of small and medium-sized enterprises. This paper reports the measures to secure the synchronization zone of the production process based on the general theory of relativity. All that is needed to perform the synchronization is to increase the deviation value of the production field. It is the production mass which greatly affects this deviation value. In the application of relativity, the mass is introduced as a parameter derived from mean and volatility. That mass is the value of the production system. We chose Riemannian space as a suitable space for calculating this mass. As numerical examples, we provide two examples of the production flow process (PFP) system and one-dimensional asymmetric simple exclusion process (ASEP) system.*
Keywords: Synchronization zone, Theory of relativity, Normal distribution, Riemannian space

1. **Introduction.** The authors have reported mathematical modeling of production processes, estimation of the production status of each process, optimal control problems, and flow analysis in small and medium scale [1, 2, 3, 4, 5, 6]. We have constructed the state in which the production density of each process corresponds to the physical propagation of heat [2, 7]. Using this approach, we have shown that the diffusion equation dominates the manufacturing process. In other words, when minimizing the potential of the production field (stochastic field), the equation, which is defined by the production density function and the boundary conditions, is described using the diffusion equation with advection to move in transportation speed. The boundary conditions mean the closed system in the production field. The adiabatic state in thermodynamics represents the same state [2, 7].

Regarding the optimal production capacity, we have reported that the quantity produced is proportional to the rate of return, which aids corporate development and limits production capacity. Therefore, we have employed the Hamilton-Jacobi-Bellman equation to calculate optimal production capacity and determine optimal parameters of the quadratic form evaluation function based on the optimal production capacity [8]. Then, we have investigated a method for optimal control of production processes that include lead-time delays. We have proposed the model that expresses lead-time lag in a strict mathematical model and the model with lead-time delay based on the average regression

DOI: 10.24507/ijicic.19.01.101

process, which is the Ornstein-Uhlenbeck process model that is used in mathematical finance. Optimal control is obtained using each state equation [9]. Also, the previous research applying fluid mechanics to the trial production of a new concept vertical take-off and landing rotorcraft of flexible kite wing attached multicopter is very interesting [10].

This is of interest that to reduce the frequency of information exchange between the controller and the system, a unique event-triggered mechanism is employed to guarantee that the criterion of exponential synchronization holds. The design of the system can be designed quite simply by the introduction of the concept of exponential synchronization [11]. Regarding the throughput model for a production flow system, we have introduced the Riemannian manifold, which is easier to implement than stochastic modeling methods [4, 5]. This model is derived from the stochastic throughput model for producing the propagation necessary to measure synchronization. We have also introduced the Fisher information matrix to specify volatility. To validate the new method and clarify the synchronization processes, we perform a dynamic simulation of the production system. We have also presented the real synchronous and asynchronous data obtained from the production flow process. No other research has introduced Riemannian manifold to demonstrate the superiority of synchronous production systems. Furthermore, we have clarified that the geometric structure of the production space, which consists of production steps and workers, should be described. Then the discussion went on about the production space like the Riemannian space.

As far as applying general relativity is concerned, there are few reports. GPS (Global Positioning System) uses satellite position and time information to calculate your location. If the satellite time information is different from 1 microsecond, it will cause an error of 300 m on the ground, so accurate information is required [12]. Naturally, numerous reports have been produced in the field of physics. We have challenged this task in the production processes. By defining the production mass, it was found that if the synchronous eigenmas increase, the process improvement can be performed to calculate the asynchronous boundary parameters according to the improvement process. This means improving performance by improving the process. Generally, the speed of light is invariant in the theory of relativity, but in the production system, the target is the target point, and it is not impossible even if the requirements of the production system change [13].

In this study, to secure the synchronization zone of the production process based on the general theory of relativity, it is necessary to improve the deviation value of the production field, and the measures are reported. We present the superiority of a synchronic production system based on the general theory of relativity. The mean value is the productivity trend, and one of the volatilities is the interest rate for government bonds in the economy, that is, the safe interest rate rate. These statistical parameters allow to calculate the throughput. In the application of relativity, the center of mass is introduced as a parameter derived from the mean value and volatility. Therefore, the central mass is defined within the Riemannian space. We regard the quantum field as equivalent to a production field, and the probability distribution of the throughput of a production field with an arbitrary region is assumed to have zero potential in the Schrodinger equation. We got a normal distribution around the original. If this is the case, the polar coordinates are constructed at an arbitrary point by rotating it at an angle around the origin. To conclude, in the one-dimensional space-time of Minkowski in the production system, the production volume increases linearly with the throughput. Usually, in the theory of relativity, the speed of light is invariant, but in a production system, the throughput corresponding to the speed of light is variable. The target point that depends on that throughput can be modified by changing the conditions of the production system.

Regarding the numerical examples, we use the ASEP to improve the efficiency of the production process [14, 15]. When applied as a model of a lot production system, the ASEP is fundamentally a nonlinear system represented by Burgers equation. This indicates that the process transition probability plays an important role. From the experience of three test runs of PFP, we make the processes of each process identical and choose the appropriate value. We arrange the workers in each process appropriately. From the aforementioned procedure, a highly linear system is obtained that approaches a stationary system. Minemura and Nishinari proposed the ASEP model and the result of theoretical solution was consistent with the simulation result [15]. The validity of the theoretical solution was confirmed. We apply the ASEP model to the actual production process, and also we represent the actual data compared with the production flow process (PFP). Comparing actual data on ASEP and PFP production efficiencies, ASEP was able to double the throughput and reduce production costs by 20%.

We are introducing a field of relativist production. This field of production is defined in Riemannian space. The production density is modeled by a stochastic differential equation. This has already been reported in a previous study. Its stochastic solution has a normal probability density function. We also present the formulation of a dynamic system for the yield potential of the production domain. In addition, a spherical symmetrical coordinate system is introduced. We are looking for solutions for production densities within the polar co-ordination system. This solution is similar to that offered by Schwarzschild. The following three points are conditions for relativist arguments.

- In 3D, the production site is in a polar coordination system.
- The potential of production site is not dependent on time.
- Infinitely (beyond the capacity of the production site), the Minkowski metric is used. Finally, it is possible to increase the output field deviation value by reducing the central potential. In other words, it becomes possible to enlarge the area in which the synchronisation of the production process can be reached.

The flow of the entire paper is as follows.

- Introduce the deviation of the distance from the synchronization point and the deviation of the phase in the production field in Riemannian space.
- By introducing both parameters, we present that the production density that goes through the production process has a normal probability distribution.
- The throughput function of the production process forms a standard normal distribution, and this function is considered as the synchronous potential. Here, we map it to the dynamic field. In the dynamic field, it forms a potential.
- Mention the effects of distance and phase deviations on the production mass of the production field. The production mass metric tensor was achieved using the metric tensor. To maximize the potential, the mass of production must be minimized. In other words, we conclude that this leads to the realization of the synchronization.

See Appendix B for an overview of the graphs and equations in the manuscript except the equations in Appendix.

2. **Production Business of a Small-to-Midsize Firm.**

2.1. **Production systems in the production equipment industry.**

We refer to the production system in manufacturing equipment industry studied in this paper. This is not a special system, but "Make-to-order system with version control". Make-to-order system is a system which allows necessary manufacturing after taking orders from clients, resulting in "volatility" according to its delivery date and lead time. In addition, "volatility" occurs in lead time depending on the contents of make-to-order products (production equipment).

However, effective utilization of the production forecast information on the orders may suppress certain amount of "variation", but the complete suppression of variation will be difficult. In other words, "volatility" in monthly cash flow occurs and of course influences a rate of return in these companies. Production management system, suitable for the separate make-to-order system which is managed by numbers assigned to each product upon order, is called as "product number management system" and is widely used. All productions are controlled with numbered products and instructions are given for each numbered product.

Thus, ordering design, logistics and suppliers are conducted for each manufacturer's serial numbers in most cases except for semifinished products (unit incorporated into the final product) and strategic stocks. Therefore, careful management of the lead time or production date may not suppress "volatility" in manufacturing (production). The company in this study is the "supplier" in Figure 1 and "factory" here. In Figure 1(A), the "Customer side" refers to an ordering company and "Supplier (D)" means the target company in this paper. The product manufacturer, which is the source of the ordered production equipment, presents an order that takes account of the market price. In Figure 1(B), the market development department at the customer's factory receives the order through the sale contract based on the predetermined strategy. This is the data actually measured by Customer and Manufacturer (to be researched) shown in Figure 1. It presents the production process data that received an order for a particular customer out of several existing customers. The client is a major semiconductor manufacturer. We have a long history of producing equipment.

2.2. **Production flow system.** A manufacturing process that is termed as a production flow process is shown in Figure 2. The production flow process, which manufactures low volumes of a wide variety of products, is produced through several stages in the production process. In Figure 2, the processes consist of six stages. In each step S1-S6 of the manufacturing process, materials are being produced by one worker of each step

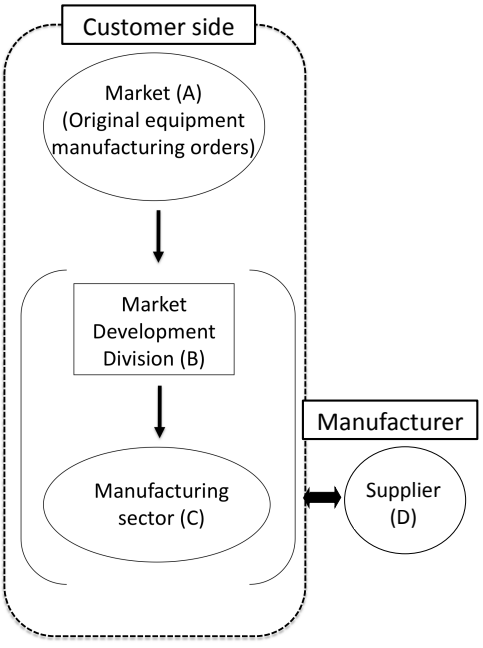

FIGURE 1. Business structure of the target company

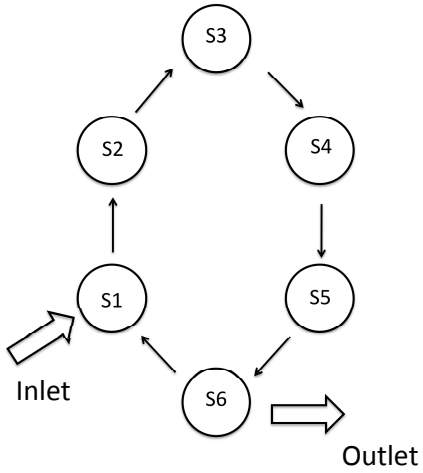

FIGURE 2. Production flow process

S1 through S6. S1-S6, which are given by Tables 6 and 8 in Appendix A, correspond to the process in Figure 2. The throughput will vary greatly depending on the proficiency level of the worker (Testrun1 and Testrun2 in Appendix A). Testrun1 and Testrun2 are an asynchronous and a synchronous process, respectively. The direction of the arrow represents the direction of the production flow. In this system, production materials are supplied from the inlet and the end product will be shipped from the outlet.

Assumption 2.1. *The production structure is nonlinear.*

Assumption 2.2. *The production structure is a closed structure; that is, the production is driven by a cyclic system (production flow system).*

- Reasonability of Assumption 2.1. Assumption 2.1 indicates that the determination of the production structure is considered a major factor, which includes the generation value of production or the rate of return generation structure in a stochastic manufacturing process (hereafter called the manufacturing field). Because such a structure is at least dependent on the demand, it is considered to have a nonlinear structure. Because the value of such a product depends on the rate of return, its production structure is nonlinear. Therefore, Assumption 2.1 reflects the realistic production structure and is somewhat valid.
- Reasonability of Assumption 2.2. Assumption 2.2 is completed in each step and flows from the next step until stage S6 is completed. Assumption 2.2 is reasonable because new production starts from S1. For a more detailed analysis, please refer to our Appendix A.

2.3. **Mathematical model for ASEP production processes.** The ASEP is a non-equilibrium statistical mechanics model that is referred to as an exclusive process. It is a simple model in which numerous particles diffuse under the volume-exclusion interaction on a one-dimensional lattice. Figure 3 shows a one-lot-flowing model in ASEP. The terms α and β denote the input and output rates, respectively, and p denotes the transition probability from one stage to another.

Figure 4 shows that the flow volume Q in the steady state changes its behavior in accordance with the magnitude relation of α, β, and p. It is determined as shown in Figure 4. In Figure 4, the flow volume is defined as follows [15]:

$$Q = \alpha \frac{p-\alpha}{p-\alpha^2}, \quad in \quad A$$

$$Q = \beta \frac{p-\beta}{p-\beta^2}, \quad in \quad B$$

$$Q = \frac{1-\sqrt{1-p}}{2}, \quad in \quad C$$

According to our previous study, we obtain the Burgers equation as follows [16]:

$$\frac{\partial S(t,x)}{\partial t} + S(t,x)\frac{\partial S(t,x)}{\partial x} = D\frac{\partial^2 S(t,x)}{\partial x^2} \tag{1}$$

where $S(t,x)$ is a production density.

Equation (1) denotes the phenomenon of turbulence in fluid dynamics. If we apply it to a production process, in the asynchronous state, the dynamic characteristics of the potential (production density) in the process are strictly nonlinear [16].

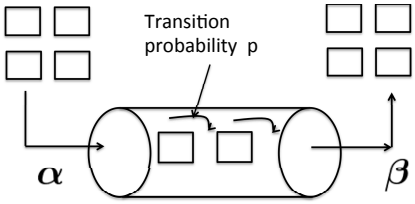

FIGURE 3. ASEP model

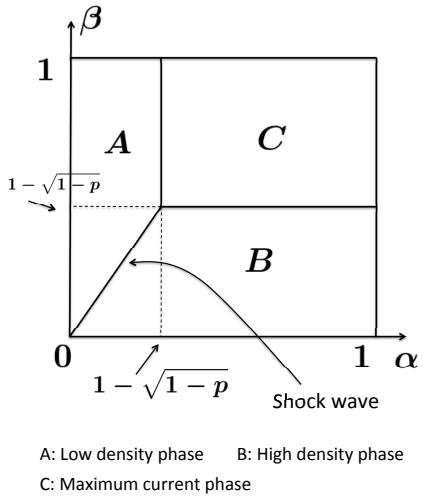

FIGURE 4. Phase diagram

We obtain the following after executing the Cole-Hopf transformation for Equation (1) [16]:

$$\frac{\partial \varphi(t,\xi)}{\partial t} = D\frac{\partial^2 \varphi(t,\xi)}{\partial \xi^2} \tag{2}$$

where $\varphi(t,\xi) \leq 1$ and $\varphi(t,\xi)$ denotes a new production density function with synchronous states and D denotes a production flow coefficient.

We obtain the solution $S(t,x)$ as follows [17]:

$$S(t,x) = -2D\frac{\partial}{\partial x}\ln\left[(4\pi Dt)^{-\frac{1}{2}}\int_{-\infty}^{\infty}\exp\left\{-\frac{(x-x')^2}{4Dt} - \frac{1}{2D}\int_0^{x'} S(0,x'')dx''\right\}dx'\right] \tag{3}$$

where the initial value $S(0,x)$ is assumed to be given, x' and x'' are first derivative and second derivative, respectively.

From Equation (2), $\varphi(t,\xi)$ is derived at infinity as follows [17]:

$$\varphi(t,\xi) = \exp\left(-\int S(t,\xi)d\xi\right) \tag{4}$$

Equation (4) represents the fact that the spatial elements or components of the nonlinear function $S(t,\xi)$ are summed and that they decay exponentially. From the perspective of production processes, Equation (4) linearizes the nonlinear characteristics of workers and aligns them according to the production processes, linearize and synchronize by process improvement. In other words, Equation (4) converts a nonlinear function into a probability distribution with an exponential family of linear functions.

Section 2 reviews using actual data. Actual data were obtained in production flow system and ASEP models. In our previous research, we have pointed out that the synchronous production process produces maximum efficiency in the production process of small and medium-sized companies. Section 3 presents the theoretical development of the application of general relativity to the productive process. Ultimately, it will signal that the area of the production field that reaches synchronization will increase.

3. **General Relativity and Production Process.**

Einstein's equation is given by

$$R_{\sigma\varphi} - \frac{1}{2}g_{\sigma\varphi}R = \frac{8\pi G}{C^4}T_{\sigma\varphi} \tag{5}$$

where $T_{\sigma\varphi}$ is the energy momentum tensor of the body that is the source of gravity [18]. R is a Ricci scalar representing the space-time geometry. $R_{\sigma\varphi}$ is a Ricci tensor. G is a gravity. C is the speed of light.

Using a tensor space with contravariant and covariant vectors, the relativistic production field $\{S_{ij}\}$ is given by the following equation.

$$S_{ij} = S_j^i e_i \otimes f^j, \quad i, j = 1, 2, 3 \tag{6}$$

Moreover, in our previous research, the throughput model in a stochastic field (time and space variables) is given by the following equation [3].

$$\partial S = \mathcal{L}_x S \partial t + \sigma \partial W \tag{7}$$

where $\mathcal{L}_x$ is a diffusion operator. W is a winner process.

Here, we make the following assumptions. This assumption looks at the production process as linear [19].

$$S(t, x) = s(t)\varphi(x) \tag{8}$$

where $s(t)$ is the throughput function with respect to time t. $\varphi(x)$ is a distribution function.

Also, the throughput function $s(t)$ is given by the stochastic differential equation below.

$$ds(t) = \mu dt + \sigma dW \tag{9}$$

where μ and σ are a trend parameter and volatility, respectively.

Here, the general theory of relativity and the production process in the production field are described. The following parameters are defined within the production field $\{S\}$.

Definition 3.1. *M: Total number of processes in the production field; D: The number of synchronous processes in the total number of processes in the production field; P: The number of asynchronous processes in the total number of processes in the production field; Relationship between M, D and P: $M = D + P$.*

The stochastic model for throughput h is given by [20]

$$ds(t) = \mu dt + \sigma dW, \quad \mu = \frac{D}{M}, \quad \sigma = \frac{P}{M} \tag{10}$$

where μ and σ are an average and a volatility respectively. h is the probability density function as follows:

$$h(x) = \frac{1}{\sqrt{2\pi}\sigma} \exp\left\{-\frac{1}{2}\left(\frac{x-\mu}{\sigma}\right)\right\} \tag{11}$$

According to Appendix A, the actual data for Testrun1 and Testrun2 of the assembly line production system are shown in Table 1 as follows. The throughput function in Figure 5 is given as follows.

$$f(x) = \frac{1}{\sqrt{2\pi}} \exp\left\{-\frac{1}{2}x^2\right\}, \quad A \leqq x \leqq B, \quad x \equiv \left[\frac{P}{M}\right] \tag{12}$$

where $A \Rrightarrow P = M$, $B \Rrightarrow P = M$ and $C \Rrightarrow P = 0$.

TABLE 1. Actual data of Testrun1 and Testrun2

	M	D	P	μ	σ
Testrun1	54	38	16	0.73	0.29
Testrun2	54	47	7	0.92	0.06

The following are the content of the main variables and parameters used in the paper.

- S_0: Production mass (relative cost)
- $\rho(\sigma_0)$: Production density
- m: Production efficiency coefficient
- σ_0: Entire production field
- σ_S: Spatial distance of production field
- G: Potential conversion factor
- S_{ij}: Production tensor
- σ: Deviation from the synchronization point (distance)
- θ: Deviation from synchronization point (phase)
- t: Deviation from synchronization point $\propto h$
- h_C: In general relativity, it has to do with the speed of light. In the production field, it represents the throughput (production speed) that cannot be exceeded, and it is assumed that h_C exists.

$f(x)$ is the throughput potential in the production process. Current potential is referred to as synchronous potential. Generally, the potential is originally expressed in the dynamic domain in the case given in Figure 6 as follows. Here, S_{ij} is a production tensor in Figure 6.

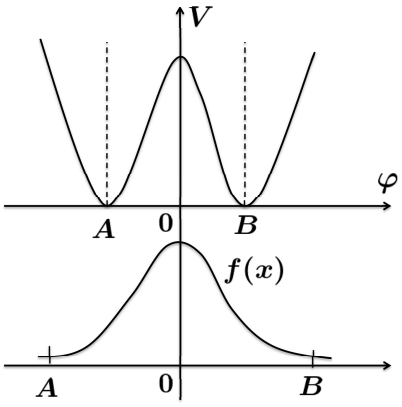

FIGURE 5. Potential (V) and throughput function ($f(x)$)

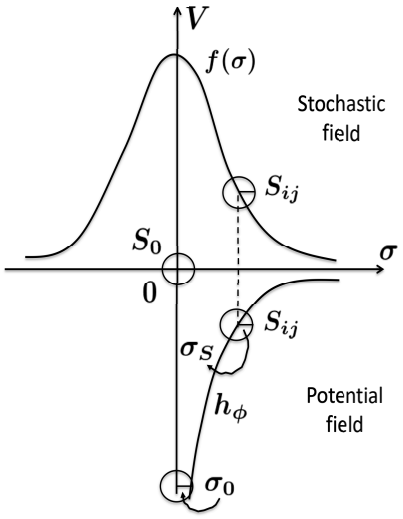

FIGURE 6. Stochastic field and potential field

Definition 3.2. *Potential h_ϕ at the origin*

$$h_\phi = -G\frac{\rho(\sigma_0)m}{\sigma} \tag{13}$$

In Figure 7, when $h(\sigma)$ revolved around the centerline, a sphere with a radius σ' is obtained in (a) cross-section. At this time, if (a) the cross section is moved up and down and fixed at an arbitrary position, a sphere having a radius σ' can be obtained in the same manner. Generally, it is considered equivalent to the productive field in the quantum field. It is assumed that the probability distribution of the throughput of the production field with an arbitrary region has zero potential in the Schrodinger equation. Under this assumption, if you have a standard normal distribution around the origin, you can form a polar coordinate system at an arbitrary point (volatility σ) by rotating it at an angular velocity around the origin. Therefore, if the production tensor on polar coordinates is set

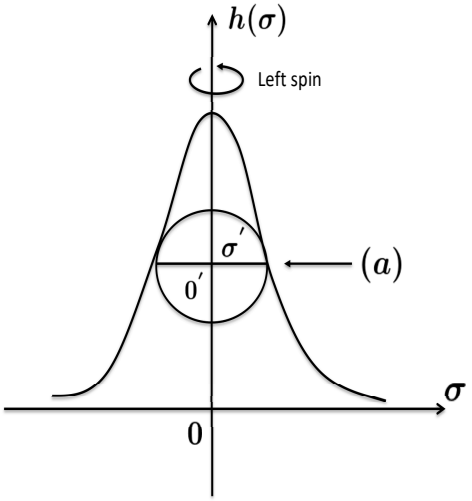

FIGURE 7. Standard normal distribution probability density function

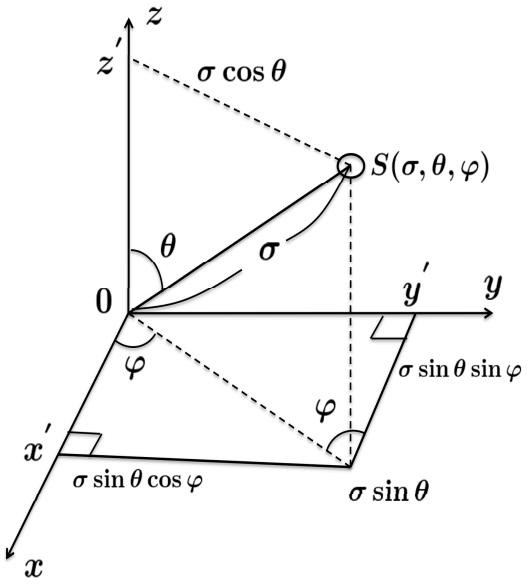

FIGURE 8. Spherical coordinate system

to S, it can be defined as $S = S(\sigma, \theta, \varphi)$ in Figure 8 in case of three dimensions. Therefore, if the potential at the origin is set at h_ϕ, the following equation can be defined. From Figure 8, the metric tensor is given by the following equation.

$$dS^2 = dx'^2 + dy'^2 + dz'^2 \tag{14}$$

where x', y', z' are given as follows:

$$x' = \sigma \sin\theta \cos\varphi, \quad y' = \sigma \sin\theta \sin\varphi, \quad z' = \sigma \cos\theta \tag{15}$$

The total derivatives of x', y', z' are given by the following equations.

$$dx' = \sin\theta \cos\varphi d\sigma + \sigma \cos\theta \cos\varphi d\theta - \sigma \sin\theta \sin\varphi d\varphi \tag{16}$$

$$dy' = \sin\theta \sin\varphi d\sigma + \sigma \cos\theta \sin\varphi d\theta + \sigma \sin\theta \cos\varphi d\varphi \tag{17}$$

$$dz' = \cos\theta d\sigma - \sigma \sin\theta d\theta \tag{18}$$

Equation (19) is obtained by substituting Equations (16), (17) and (18) into Equation (14).

$$dS^2 = d\sigma^2 + \sigma^2 d\theta^2 + \sigma^2 \sin\theta^2 d\varphi^2 \tag{19}$$

where the terms $d\sigma d\theta$, $d\theta d\varphi$ and $d\sigma d\varphi$ are set to zero.

4. Gravity Field Equations for Production Processes.

4.1. **Sample application on a batch production field.** In a batch production field, it is assumed that production mass cost is the only one in the center. In addition, the model of co-ordinates of the production field is based on a system of spherically symmetrical co-ordinates. The tensor space requirements are outlined below.

- In three dimensions, the production field is a system of spherically symmetrical co-ordinates.
- The potential of the production field must not depend on time.
- At the point to infinity, that is beyond the power of the production plant, this is Minkowski weights.

The linear system is given by the following equation by Minkowski space-time and spherically symmetric coordinates [18]. Please refer to the Appendix B for the meaning of Equation (20).

$$dS^2 = -\exp(v(\sigma))dt^2 + \exp(\lambda(\sigma))d\sigma^2 + \sigma^2 d\theta^2 + \sigma^2 \sin\theta^2 d\varphi^2 \tag{20}$$

where v ($v \ll C$) and σ are the advection speed and the process size respectively. C is the speed of light.

The solution to Equation (20) is provided by [18, 21]

$$dS^2 = -\left(1 - \frac{2m}{v^2\sigma}\right) v^2 dt^2 + \left(\frac{1}{1 - \frac{2m}{v^2\sigma}}\right) d\sigma^2 + \sigma^2 d\theta^2 + \sigma^2 \sin\theta^2 d\varphi^2 \tag{21}$$

where the term $\left(1 - \frac{2m}{v^2\sigma}\right)$ is the trend factor for t and σ. $v^2 \ll C^2$. v is the advection velocity.

In the case of a batch production system, a mass (cost) exists at the centre. Here, σ_S is given as follows.

$$\sigma_S = \frac{2G\rho(\sigma_0)m}{v^2} = 2G\frac{\rho(\sigma_0)m}{\left(\rho(\sigma_0)m/T\right)^2} \tag{22}$$

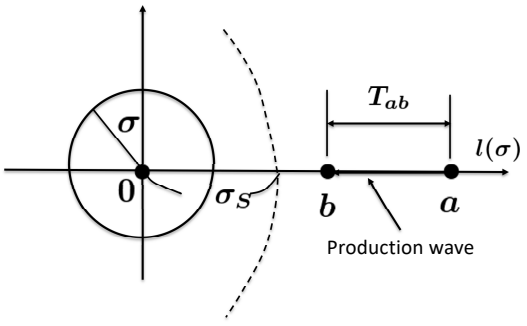

FIGURE 9. Mass (cost) existing at the centre in a batch production system

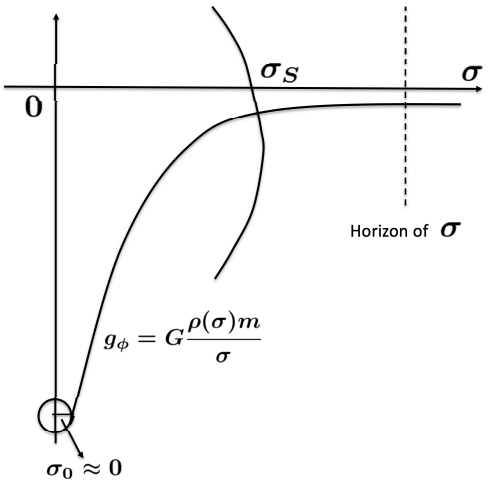

FIGURE 10. Potential function h_ϕ in the production field

For the moment, the deviation from the synchronization point (distance) σ_S can be changed as follows.

$$\sigma_S = \frac{T_S}{v_S} \cdot \frac{2G}{\rho(\sigma_0)m}, \;\; \Rrightarrow \sigma_S \cong \frac{T_S}{v_S}, \;\; \rho(\sigma_0)m \equiv Constant, \;\; M, D, P : Constant \tag{23}$$

where v_S and T_S are the advection speed and the total lead time in production field, respectively.

Increasing the gradient of advection velocity with respect to lead time decreases r_S. This means that increased throughput reduces the marginal cost. That is, in physics, the part where $\sigma \leqq \sigma_S$ is called a black hole. Therefore, in the area of production, mass (cost) cannot exceed the maginal cost of simultaneously completing this part (Black hole conditions at the production field). However, this is the only case where the production does not exist in the field. As a result, it does not apply to production field where every production mass (cost) is organically combined.

Here, σ is set by the following equation.

$$\sigma = \frac{T}{v}\left(\frac{2G}{\rho(\sigma_0)m}\right) \tag{24}$$

So, if the metric tensor is considered as Equation (20), the above analysis stands. The Schwartzschild solution (the solution of the Einstein equation) is as follows. However, it is spherically symmetric and is an exact solution in a vacuum [21].

$$dS^2 = -\left(1 - G\frac{2\rho(\sigma_0)m}{\sigma_C^2\sigma}\right)\sigma_C^2 dt^2 + \left(\frac{1}{1 - \frac{2\rho(\sigma_0)m}{\sigma_C^2\sigma}}\right)dr^2 + \sigma^2 d\theta^2 + \sigma^2 \sin\theta^2 d\varphi^2 \tag{25}$$

4.2. **Analysis of the production field with metric tensioners.** From Equation (25), we obtain the following solution in the polar coordinates.

$$dS^2 = -(1-D)\sigma_C^2 dt^2 + \frac{1}{1-D}d\sigma^2 + \sigma^2 d\theta^2, \quad D = \frac{2G\rho(\sigma_0)m}{\sigma_C^2 \cdot \sigma} \tag{26}$$

Equation (26) (solution) is similar to Schwarzschild's solution under special conditions in the general theory of relativity [22].

Currently, if $\sigma_C = 1$, the following equation is available.

$$dS^2 = -\left(1 - \frac{2G\rho(\sigma_0)m}{\sigma}\right)dt^2 + \left(\frac{1}{1 - \frac{2G\rho(\sigma_0)m}{\sigma}}\right)d\sigma^2 + \sigma^2 d\theta^2 \tag{27}$$

We get the following values by presenting a numerical example in Equation (27).

$$m = \left(1 - \frac{M_0}{M}\right) = 1.0 \;\; (M_0 = 0) \tag{28}$$

$$G = 0.5 \;\; (\sigma_C = 1.0,\; m = 1.0,\; \rho(\sigma_0) = 1.0) \tag{29}$$

From Equations (28) and (29), the following equation is obtained:

$$\sigma = 2G\rho(\sigma_0)m, \;\; \Leftarrow \left(1 - \frac{2G\rho(\sigma_0)m}{\sigma}\right) = 0 \tag{30}$$

In this case, σ diverges to infinity. $\sigma = \sigma_S$ is known to match the horizon of a radial symmetric static black hole and is called the Schwartzschild radius [18, 21].

5. **Numerical Examples.** The fundamental principle of our numerical calculation is that we can accurately reflect dynamic systems. Many existing reports deal with static mathematical models. Real dynamic behaviour can be verified without comparison, and system optimization and efficiency can be proposed according to reality. We present the numeric values of the production method presented in Section 5. The final products of PFP and ASEP are respectively 6 and 12, and the theoretical throughput is 400 (min) and 400 (min) respectively [14]. Regarding with the final products of PFP and ASEP, please refer to the advance research for details [14].

Next, we set the value of m to identify σ_S.

$$\sigma_S = 2G\rho(\sigma_0)m = 2 \times 0.5 \times 1.0 \times m, \;\; \Rrightarrow \frac{M_0}{M} = 0.7 \Rrightarrow \;\; m = 0.3, \;\; \Rrightarrow \sigma_S = 0.3 \tag{31}$$

5.1. **Evaluation of numerical examples.** $\rho(\sigma_0)$ and m $(= 1 - M_0/M)$ shown in the numerical example represent the mass density and the process mass, respectively. $\rho(\sigma_0)$ includes fixed cost. If $\rho(\sigma_0)$ and m fall, σ_S falls. In other words, the volatility is linked not

TABLE 2. Value of M_0 and M related PFP and ASEP

Testrun number	Production process	M_0	M
Testrun1	Asynchronous process	16	54
Testrun2	Synchronous process	7	54
Testrun1 (ASEP)	Asynchronous process	16	60
Testrun2 (ASEP)	Synchronous process	17	60
Testrun3 (ASEP)	Synchronous process	20	60

TABLE 3. Evaluation value of σ_S of PFP and ASEP

Production method	Test method	σ_S
PFP	Testrun1	0.29
PFP	Testrun2	0.12
ASEP	Testrun1	0.26
ASEP	Testrun2	0.28
ASEP	Testrun3	0.33

only to the capacity of the process, but also to the density of the production mass. In addition, $\rho(\sigma_0)$ is defined as the following function.

Definition 5.1. *Production efficiency function* $\rho(\sigma_0)$

$$\rho(\sigma_0) \equiv \rho(\sigma_0, \alpha, \beta) \tag{32}$$

where σ_0, α, β are the process lead time volatility, the cost rate and the labor cost rate respectively. Figure 11 shows that $g(\sigma_0)$ shifts to the left and right to the center of γ depending on the ratio of γ. So the global model is Equation (38) that takes the ratio into account. Figure 12 shows the provability density function $\varphi(\xi)$, which is expressed by the following equation.

$$\varphi(\xi) = \frac{1}{\sqrt{2\pi}\sigma} \exp\left(-\frac{1}{2}\left(\frac{\xi-\mu}{\sigma}\right)^2\right) \tag{33}$$

Here, $g(\sigma_0)$ is given by the following equation.

$$g(\sigma_0) = \gamma \int_0^\infty \varphi_{+\alpha}(\xi)d\xi + (1-\gamma)\int_0^\infty \varphi_{-\alpha}(\xi)d\xi \tag{34}$$

where $\varphi_{+\alpha}$ and $\varphi_{-\alpha}$ are as follows:

$$\varphi_{+\alpha} = \frac{1}{\sqrt{2\pi}\sigma_0} \exp\left(-\frac{1}{2}\left(\frac{\xi-(\gamma+\alpha)}{\sigma_0}\right)^2\right) \tag{35}$$

$$\varphi_{-\alpha} = \frac{1}{\sqrt{2\pi}\sigma_0} \exp\left(-\frac{1}{2}\left(\frac{\xi-(\gamma-\alpha)}{\sigma_0}\right)^2\right) \tag{36}$$

Consequently, if the intrinsic density is set at $m(\sigma_0)$, we define $\rho(\sigma_0)$ as the following equation.

$$\rho(\sigma_0) = (1 - g(\sigma_0))m(\bullet) \tag{37}$$

where $m(\bullet)$ is the intrinsic mass density.

In reality, the rate of decrease in $(1 - g(\sigma_0))$ can be expected (assuming $m(\bullet) = 1.0$).

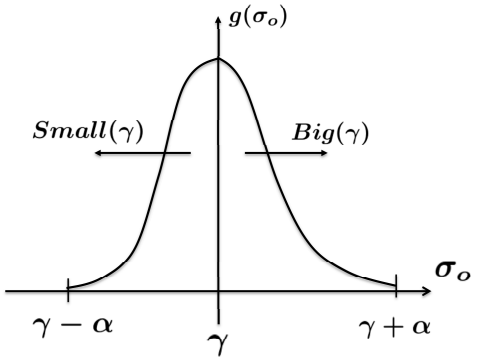

FIGURE 11. Probability distribution function

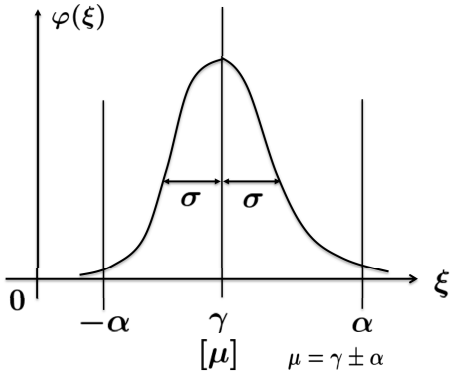

FIGURE 12. Probability density function

In this case, if we rewrite $g(\sigma_0)$, we get the following equation.

$$g(\sigma_0) = 1 - \left\{\gamma\Phi\left(\frac{\gamma+\alpha}{\sigma_0}\right) + (1-\gamma)\Phi\left(\frac{\gamma-\alpha}{\sigma_0}\right)\right\} \tag{38}$$

where $\Phi(\bullet)$ is the standard normal distribution density function [3].

The graphics created from Equation (38) are Figure 13 and Figure 14.

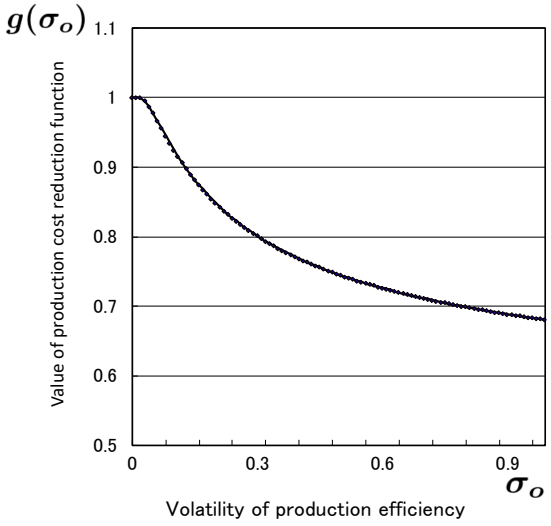

FIGURE 13. Value of the function of reducing production costs ($M = 54$, $D = 47$, $P = 7$)

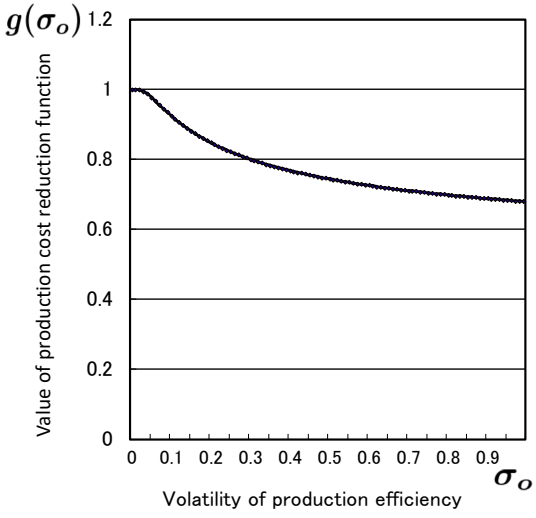

FIGURE 14. Value of the function of reducing production costs ($M = 54$, $D = 38$, $P = 16$)

Regarding the maximum production point reduction rate, these values in Figures 13 and 14 are 0.8333 and 0.7881 relatively. In Figure 13, the average value (γ) of production efficiency is 0.5, which is a 10% decrease. In Figure 14, the average value (γ) production efficiency is 0.5, which is a 20% decrease. We aim to produce at a 10% reduction rate.

TABLE 4. Parameter values of Figures 13 and 14

Figure number	M	D	P	Average value (γ)	Volatility (α)
Figure 13	54	47	7	0.8704	0.1296
Figure 14	54	38	16	0.7037	0.2963

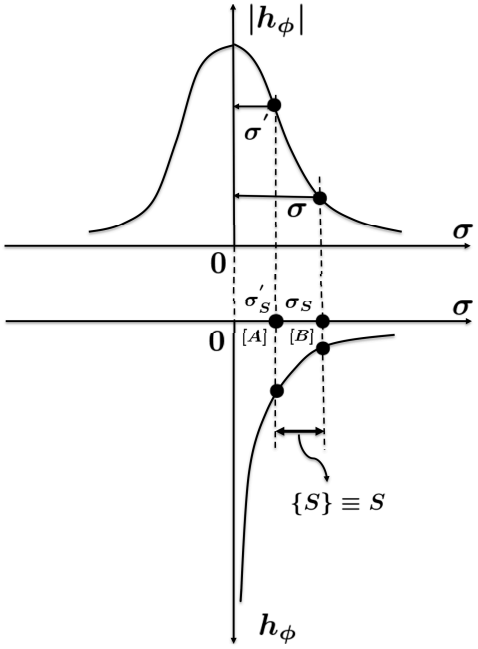

FIGURE 15. Deviation value of standard normal distribution

The magnitude of σ_0 can be regarded as the difference in the synchronization of the product, that is, the value of deviation of the synchronization. When σ_0 takes a large value, the drift value of the synchronization approach becomes low.

In Figure 15, the value of the deflection of point A ($\sigma'_S = 0,1$) is 63, and the value of the deflection of point B ($\sigma_S = 0,3$) is 55.

On the basis of the aforementioned results, the following equation is obtained.

$$\sigma_S = 2G\rho(\sigma_0)\{1 - g(\sigma_0)\}m/\sigma_C^2, \quad m = \left(1 - \frac{D}{M}\right) \tag{39}$$

where $g(\sigma_0)$ is given as Equation (38). σ_C is a limit value of synchronization deviation value.

Now, when $\sigma_0 \approx 0.5$ and $\sigma_C = 1.0$, $g(\sigma_0) \approx 0.9$. Therefore, if σ_S is positioned as shown in the next equation, it is similar to the Schwarzschild solution.

σ_C is set to 1.0 because it is set to a standardized value. σ_0 is set to a value as close to zero as possible. This setting results in σ_S ranging from $0.29 \leq \sigma \leq 0.33$.

$$\sigma_S = \frac{2GM}{\sigma_C^2}, \quad M \equiv \rho(\sigma_0)\{1 - g(\sigma_0)\}m \tag{40}$$

M is then called the mass of production. Furthermore, $\rho(\sigma_0)$ is known as production density. σ_S is the value at the maximum potential of the product when $\rho(\sigma_0) = 1.0$ and $m = 1.0$. Furthermore, since M can be reduced by improving the efficiency of the production field, σ'_S ($< \sigma_S$) can be carried out as shown in Figure 15. In other words, it means that the zone of the production field where the synchronization is performed becomes large. σ_S is called a synchronous safety line. Consequently, by reducing the central potential (improving efficiency), the deflection value of the production field can be increased.

6. **Conclusion.** We reported the measures to secure the synchronization zone of the production process based on the general theory of relativity. We have already reported that synchronization is achieved to improve production efficiency. In this paper, it is possible

to increase the deviation value of production efficiency by reducing the production mass. In other words, the synchronization zone of the production field can be increased. As a result, it was found that it leads to the realization of improvement in production efficiency. Next time, we will report that the fact that the throughput has a standard normal distribution can be obtained approximately by the Schrodinger equation in quantum mechanics when the potential of the production field is set to zero.

REFERENCES

[1] K. Shirai, Y. Amano and T. Uda, Manufacture allocation of the batch process and the cyclic flow process via stochastic analysis, *International Journal of Innovative Computing, Information and Control*, vol.16, no.3, pp.939-954, 2020.

[2] K. Shirai, Y. Amano and A. Ando, Analytical mechanics approach to conservation in production field, *International Journal of Innovative Computing, Information and Control*, vol.17, no.1, pp.67-91, 2021.

[3] K. Shirai, Y. Amano and T. Uda, Cost reduction function considering stochastic risks in the production process, *International Journal of Innovative Computing, Information and Control*, vol.16, no.4, pp.1257-1278, 2020.

[4] K. Shirai and Y. Amano, Use of a Riemannian manifold to improve the throughput of a production flow system, *International Journal of Innovative Computing, Information and Control*, vol.12, no.4, pp.1073-1087, 2016.

[5] K. Shirai, Y. Amano, A. Ando and T. Uda, Spatial properties of production flow system based on Riemannian manifold structure, *International Journal of Innovative Computing, Information and Control*, vol.17, no.3, pp.831-851, 2021.

[6] K. Shirai, Y. Amano, A. Ando and T. Uda, Evaluation of production flow system utilizing expected high volume effective rate, *International Journal of Innovative Computing, Information and Control*, vol.17, no.4, pp.1203-1224, 2021.

[7] H. Tasaki, *Thermodynamics – A Contemporary Perspective (New Physics Series)*, Baifukan Co., LTD., pp.20-80, 2000.

[8] K. Shirai and Y. Amano, An optimal production capacity control including outside suppliers, *International Journal of Innovative Computing, Information and Control*, vol.13, no.1, pp.167-182, 2017.

[9] K. Shirai and Y. Amano, Optimal control of production processes that include lead-time delays, *International Journal of Innovative Computing, Information and Control*, vol.15, no.1, pp.21-37, 2019.

[10] K. Hayama and H. Irie, Trial production of kite wing attached multicopter for power saving and long flight, *ICIC Express Letters, Part B: Applications*, vol.10, no.5, pp.405-412, 2019.

[11] X. Sun and X. Song, Dissipative analysis and event-triggered exponential synchronization for fractional-order complex-valued reaction-diffusion neural networks, *International Journal of Innovative Computing, Information and Control*, vol.18, no.5, pp.1519-1536, 2022.

[12] T. Fukuyama, About GPS special and general phase compensation, *The Institute of Systems, Control and Information Engineers*, vol.51, no.6, pp.255-260, 2007 (in Japanese).

[13] K. Shirai, Y. Amano, A. Ando and T. Uda, Analysis of the throughput of the production system with the aid of general relativity, *International Journal of Innovative Computing, Information and Control*, vol.18, no.4, pp.1071-1088, 2022.

[14] K. Shirai and Y. Amano, Production model using an asymmetric simple exclusion process, *International Journal of Innovative Computing, Information and Control*, vol.14, no.1, pp.65-81, 2018.

[15] T. Minemura and K. Nishinari, Improvement of production efficiency by changing number of lot in production line, *Reports of RIAM Symposium No.22AO-S8 Development in Nonlinear Wave: Phenomena and Modeling*, 2010.

[16] K. Shirai and Y. Amano, Analysis of fluctuations in production processes using Burgers equation, *International Journal of Innovative Computing, Information and Control*, vol.12, no.5, pp.1615-1628, 2016.

[17] A. Kaneko, *Introduction to Partial Differential Equation*, Tokyo University Press, 1998.

[18] K. Sato, *Theory of Relativity*, Iwanami Co., LTD., 1996.

[19] K. Shirai, Y. Amano and S. Omatu, Mathematical model of thermal reaction process for external heating equipment in the manufacture of semiconductors (Part I), *International Journal of Innovative Computing, Information and Control*, vol.9, no.4, pp.1557-1571, 2013.
[20] K. Shirai and Y. Amano, Production throughput evaluation using the Vasicek model, *International Journal of Innovative Computing, Information and Control*, vol.11, no.1, pp.1-17, 2015.
[21] H. Shinkai, *The World of General Relativity*, http://www.einstein1905.info/, 2006.
[22] M. Toda, *30 Lectures on Theory of Relativity (30 Lectures on Physics Series)*, Asakura Co., LTD., 1997.

Appendix A. Analysis of Actual Data in the Production Flow System. Based on the control equipment, the product can be manufactured in one cycle. The rate of return required to maintain 6 pieces of equipment/day is as follows.

- (Testrun1) Because the throughput of each process (S1-S6) is asynchronous, the overall process throughput is asynchronous. In Table 5, we list the manufacturing time (min) of each process. In Table 7, we list the volatility in each process performed by the workers. Finally, Table 6 lists the target time. The theoretical throughput is obtained as $3 \times 199 + 2 \times 15 = 627$ (min). In addition, the total working time in stage S3 is 199 (min), which causes a bottleneck. In Figure 16, we plot the measurement data listed in Table 6, which represents the total working time of each worker (K1-K9). In Figure 17, we plot the data contained in Table 6, which represents the volatility of the working time.

Table 5. Correspondence between the table labels and the Testrun number

	Table number	Production process	Working time	Volatility
Testrun1	Table 6	Asynchronous process	627 (min)	0.29
Testrun2	Table 8	Synchronous process	500 (min)	0.06

Table 6. Testrun1

	WS	S1	S2	S3	S4	S5	S6
K1	15	20	20	25	20	20	20
K2	20	22	21	22	21	19	20
K3	10	20	26	25	22	22	26
K4	20	17	15	19	18	16	18
K5	15	15	20	18	16	15	15
K6	15	15	15	15	15	15	15
K7	15	20	20	30	20	21	20
K8	20	29	33	30	29	32	33
K9	15	14	14	15	14	14	14
Total	145	172	184	199	175	174	181

Table 7. Volatility of Table 6

	S1	S2	S3	S4	S5	S6
K1	1.67	1.67	3.33	1.67	1.67	1.67
K2	2.33	2	2.33	2	1.33	1.67
K3	1.67	3.67	3.33	2.33	2.33	3.67
K4	0.67	0	1.33	1	0.33	1
K5	0	1.67	1	0.33	0	0
K6	0	0	0	0	0	0
K7	1.67	1.67	5	1.67	2	1.67
K8	4.67	6	5	4.67	5.67	6
K9	0.33	0.33	0	0.33	0.33	0.33

- (Testrun2) Set to synchronously process the throughput. The target time listed in Table 8 is 500 (min), and the theoretical throughput (not including the synchronization idle time) is 400 (min). Table 9 presents the volatility of each working process (S1-S6) for each worker (K1-K9). On the basis of these results, the idle time must be set to 100 (min). Moreover, the theoretical target throughput (T_s') can be obtained using the "Synchronization with preprocess" method. This goal is as follows:

$$\begin{aligned} T_s &\sim 20 \times 6 \text{ (First cycle)} + 17 \times 6 \text{ (Second cycle)} \\ &\quad + 20 \times 6 \text{ (Third cycle)} + 20 \text{ (Previous process)} + 8 \text{ (Idle-time)} \\ &\sim 370 \text{ (min)} \end{aligned} \tag{41}$$

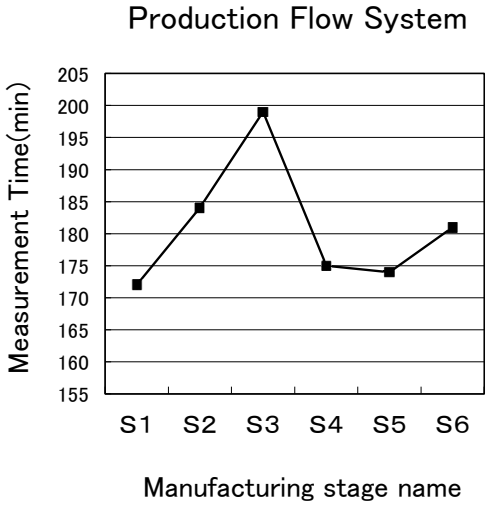

FIGURE 16. Total work time for each stage (S1-S6) in Table 6

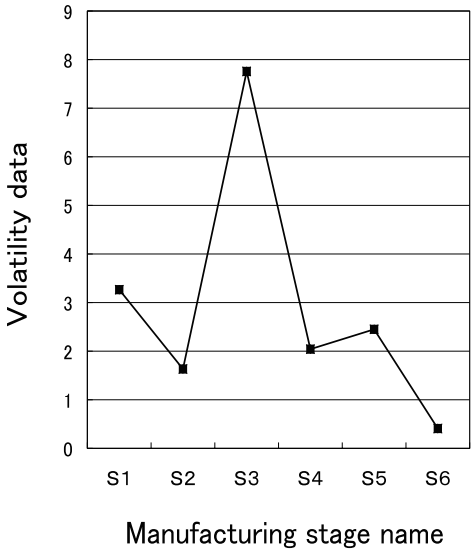

FIGURE 17. Volatility data for each stage (S1-S6) in Table 6

TABLE 8. Testrun2

	WS	S1	S2	S3	S4	S5	S6
K1	20	20	24	20	20	20	20
K2	20	20	20	20	20	22	20
K3	20	20	20	20	20	20	20
K4	20	25	25	20	20	20	20
K5	20	20	20	20	20	20	20
K6	20	20	20	20	20	20	20
K7	20	20	20	20	20	20	20
K8	20	27	27	22	23	20	20
K9	20	20	20	20	20	20	20
Total	180	192	196	182	183	182	180

TABLE 9. Volatility of Table 8

	S1	S2	S3	S4	S5	S6
K1	0	1.33	0	0	0	0
K2	0	0	0	0	0.67	0
K3	0	0	0	0	0	0
K4	1.67	1.67	0	0	0	0
K5	0	0	0	0	0	0
K6	0	0	0	0	0	0
K7	0	0	0	0	0	0
K8	2.33	2.33	0.67	1	0	0
K9	0	0	0	0	0	0

The full synchronous throughput in one stage (20 min) is

$$T'_s = 3 \times 120 + 40 = 400 \text{ (min)} \tag{42}$$

Using the "Synchronization with preprocess" method, the throughput is reduced by approximately 10%. Therefore, we showed that our proposed "Synchronization with preprocess" method is realistic and can be applied in flow production systems. Below, we represent for a description of the "Synchronization with preprocess".

Next, we manufactured one piece of equipment in three cycles. To maintain a throughput of six units/day, the production throughput must be as follows:

$$\frac{(60 \times 8 - 28)}{3} \times \frac{1}{6} \simeq 25 \text{ (min)} \tag{43}$$

where the throughput of the preprocess is set to 20 (min). In Equation (43), the value 28 represents the throughput of the preprocess plus the idle time for synchronization. Similarly, the number of processes is 8 and the total number of processes is 9 (8 plus the preprocess). The value of 60 is obtained as 20 (min) $\times$ 3 (cycles).

The results are as follows. Here, the trend coefficient, which is the actual number of pieces of equipment/the target number of equipment, represents a factor that indicates

the degree of the number of pieces of manufacturing equipment.
Testrun1: 4.4 (pieces of equipment)/6 (pieces of equipment) = 0.73,
Testrun2: 5.5 (pieces of equipment)/6 (pieces of equipment) = 0.92,
Volatility data represent the average value of each Testrun.

Appendix B. Table to Summarize Figures and Formulas in This Paper except for Appendix. Additional information on statistics parameters in Riemannian spaces.

$$\xi = \{\xi_1, \xi_2, \ldots, \xi_n\} \tag{44}$$

where $\xi_n \equiv \{t_n, \sigma_n\}$, t_n and σ_n are time and volatility, respectively.

The typical monitoring parameters are as follows.

$$\{\sigma_n(t_n), \theta_n(\sigma_n)\} \Longrightarrow \{\sigma, \theta\} \tag{45}$$

$$\sigma = \{\sigma_1, \sigma_2, \ldots, \sigma_n\}, \quad \theta = \{\theta_1, \theta_2, \ldots, \theta_n\} \tag{46}$$

where σ and θ are volatility and trend parameters, respectively.

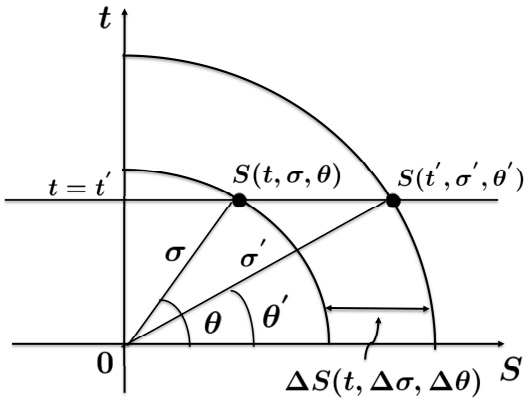

FIGURE 18. Polar space of production mass

TABLE 10. Title of figures

Figure number	Title name of figure No.
Figure 1	Business structure of the target company
Figure 2	Production flow process
Figure 3	One-lot-flowing model in ASEP
Figure 4	Phase diagram
Figure 5	Potential (V) and throughput function ($f(x)$)
Figure 6	Stochastic field and potential field
Figure 7	Standard normal distribution probability density function
Figure 8	Spherical coordinate system
Figure 9	Mass (cost) existing at the centre in a batch production system
Figure 10	Potential function h_ϕ in the production field
Figure 11	Probability distribution function
Figure 12	Probability density function
Figure 13	Value of the function of reducing production costs ($M = 54$, $D = 47$, $P = 7$)
Figure 14	Value of the function of reducing production costs ($M = 54$, $D = 38$, $P = 16$)
Figure 15	Deviation value of standard normal distribution

TABLE 11. Title of notations

Notation number	Title name of notation No.
Equation (1)	Phenomenon of turbulence in fluid dynamics
Equation (2)	Cole-Hopf transformation equation for Equation (1)
Equation (3)	Solution of Equation (1)
Equation (4)	Linearization of $S(t,x)$ with the nonlinear characteristics
Equation (5)	Einstein's equation
Equation (6)	Relativistic production field S_{ij}
Equation (7)	Throughput model in a stochastic field
Equation (8)	Assumption looks at the production process as linear
Equation (9)	Throughput function $s(t)$
Equation (10)	Stochastic model for throughput h
Equation (11)	Probability density function $h(x)$
Equation (12)	Throughput function in Figure 5
Equation (13)	Definition of the potential h_ϕ at the origin
Equation (14)	Metric tensor in Figure 8
Equation (15)	Polar coordinates transformation of x', y' and z'
Equation (16)	Term x' of Equation (14)
Equation (17)	Term y' of Equation (14)
Equation (18)	Term z' of Equation (14)
Equation (19)	This is obtained by substituting Equations (16), (17) and (18) into Equation (14)
Equation (20)	Linear system under Minkowski space-time and spherically symmetric coordinates
Equation (21)	Solution to Equation (20)
Equation (22)	In the case of a batch production system, σ_S equation
Equation (23)	Deviation from the synchronization point (distance) σ_S
Equation (24)	Deviation from the synchronization point (distance) σ
Equation (25)	Metric tensor dS^2 equation
Equation (26)	Solution of dS^2 in the polar coordinates under three dimensions
Equation (27)	dS^2 in case of $\sigma_C = 1$
Equation (28)	Numerical example in Equation (27)
Equation (29)	Same as Equation (27)
Equation (30)	Calculation of σ
Equation (31)	Value of m to identify σ_S
Equation (32)	Definition of $\rho(\sigma_0)$
Equation (33)	Provability density function $\varphi(\xi)$
Equation (34)	Probability distribution function $g(\sigma_0)$
Equation (35)	Provability density function $\varphi_{+\alpha}$ and $\varphi_{-\alpha}$ respectively
Equation (36)	Same as Equation (35)
Equation (37)	Production efficiency function $\rho(\sigma_0)$
Equation (38)	Probability distribution function $g(\sigma_0)$
Equation (39)	Value at the maximum potential of the product when $\rho(\sigma_0) = 1.0$ and $m = 1.0$
Equation (40)	Same as Equation (39)

As far as A and B are concerned from Figure 15, the metric tensor of S is given by [18]

$$dS^2 = g_{\sigma\theta} d\sigma d\theta \tag{47}$$

where $g_{\sigma\theta}$ is the Riemannian metric under S [18].

$$g_{\sigma\theta} = \begin{bmatrix} 1 & 0 \\ 0 & \dfrac{1}{\sigma^2} \end{bmatrix} \tag{48}$$

Therefore, the metric tensor on $S(t, \sigma, \theta)$ is given by

$$dS^2 = -\xi(\sigma)dt^2 + r(\sigma)d\sigma^2 + \sigma^2 d\theta^2 \tag{49}$$

In other words, the spatial setting related to dt is σ, which is also related to $d\sigma$. θ depends on the magnitude of σ. In Equation (49), by setting $\xi(\sigma) = \exp(v(\sigma))$ and $r(\sigma) = \exp(\lambda(\sigma))$ to simplify the following calculation, we get Equation (20).

Author Biography

Kenji Shirai received the B.Sc. degree in Electrical Engineering from Ritsumeikan University, Japan, 1973; the M.Sc. degree in Electrical Engineering from Ritsumeikan University, Japan, 1975; the Ph.D. degree in Electrical Engineering from Ritsumeikan University, Japan, 2000.

Dr. Shirai is engaged in research on optimal control of distributed parameter systems, modeling of industrial systems applying mathematical finance, and optimal control.

Yoshinori Amano received the B.Sc. degree in Electrical Engineering from Ritsumeikan University, Japan, 1971; the M.Sc. degree in Electrical Engineering from Ritsumeikan University, Japan, 1973; the Ph.D. degree in Electrical Engineering from Ritsumeikan University, Japan, 1977.

Dr. Amano is engaged in research on optimal control of distributed parameter systems, modeling of information systems applying mathematical finance, and optimal control. Currently, he is Advisor of Kyohnan Electric Co., LTD.

Atsuya Ando received the Dr. Eng. degree in System Information Engineering from Tsukuba University, in 2013. In 1990, he joined the Nippon Telegraph and Telephone Corporation (NTT) Wireless Systems Laboratories, Yokosuka, Japan. He was engaged in research and development of personal and base station antennas for wireless mobile communication systems. From 2000 to 2003, he was with the ATR Adaptive Communications Research Laboratories, Kyoto, Japan, engaging in research and development on adaptive array antennas for wireless ad-hoc network systems. In 2019, he moved to Niigata University of International and Information Studies, and he is currently a Professor in the Department of Information Systems. His research interests include mobile and base station antennas using metamaterials for wireless communication systems.

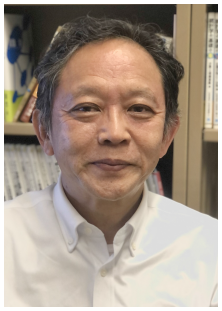

Takayuki Uda received a doctoral degree (Information Science) from the Graduate School of Information Sciences, Tohoku University, Japan, in 2009; a master's degree (Informatics) from the University of Library and Information Science (now Information and Media Studies, University of Tsukuba).

Prof. Uda is currently a full-time professor at the Department of Information Systems, Faculty of Business and Informatics, Niigata University of International and Information Studies. His research fields are data science and natural language processing. His research results contribute to the education and research of students.